

BIROn - Birkbeck Institutional Research Online

Jewell, A. and Drake, N. and Crocker, A. and Bakker, N. and Kunkelova, T. and Bristow, Charlie S. and Cooper, M. and Milton, A. and Breeze, P. and Wilson, P. (2021) Three North African dust source areas and their geochemical fingerprint. *Earth and Planetary Science Letters* 554 (116645), ISSN 0012-821X.

Downloaded from: <https://eprints.bbk.ac.uk/id/eprint/41057/>

Usage Guidelines:

Please refer to usage guidelines at <https://eprints.bbk.ac.uk/policies.html>

or alternatively

contact lib-eprints@bbk.ac.uk.

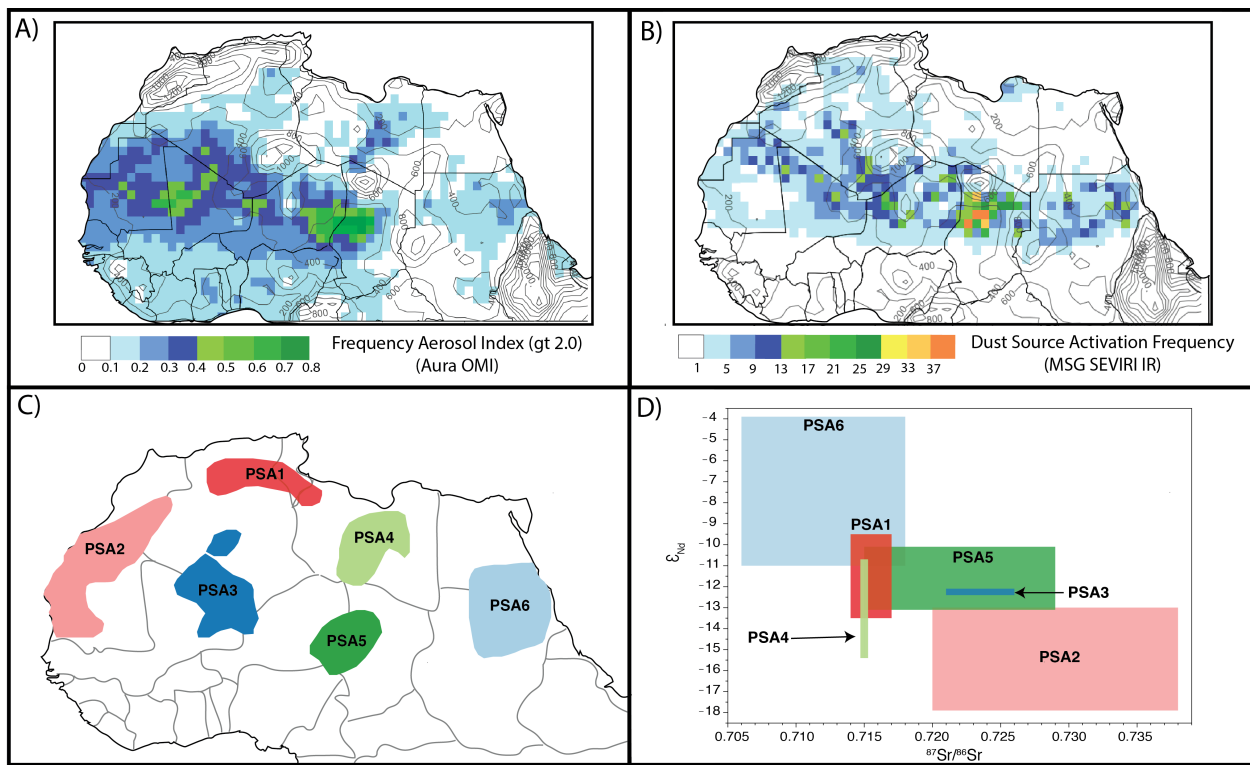


Figure 1: Previous analyses of North African preferential dust source areas (PSAs). $1^\circ \times 1^\circ$ maps of North African dust sources from March 2006 to February 2010, based on A) OMI aerosol index (Map from Schepanski et al., 2012; frequency-based remote sensing method) B) MSG SEVIRI IR dust index (Schepanski, et al., 2012; employs backtracking method therefore removing dust transport bias). C) Geographical definition of North African Potential Source Areas (PSAs) of (Adapted from Scheuven *et al.* (2013)) based on a variety remote sensing techniques that conflate dust transport and emission. D) Geochemical characterization of North African PSAs, as defined in Figure 1C, in Nd-Sr isotope space (PSAs 1 - 4 & 6 from Scheuven et al., 2013, PSA 5 from Abouchami et al., 2013).

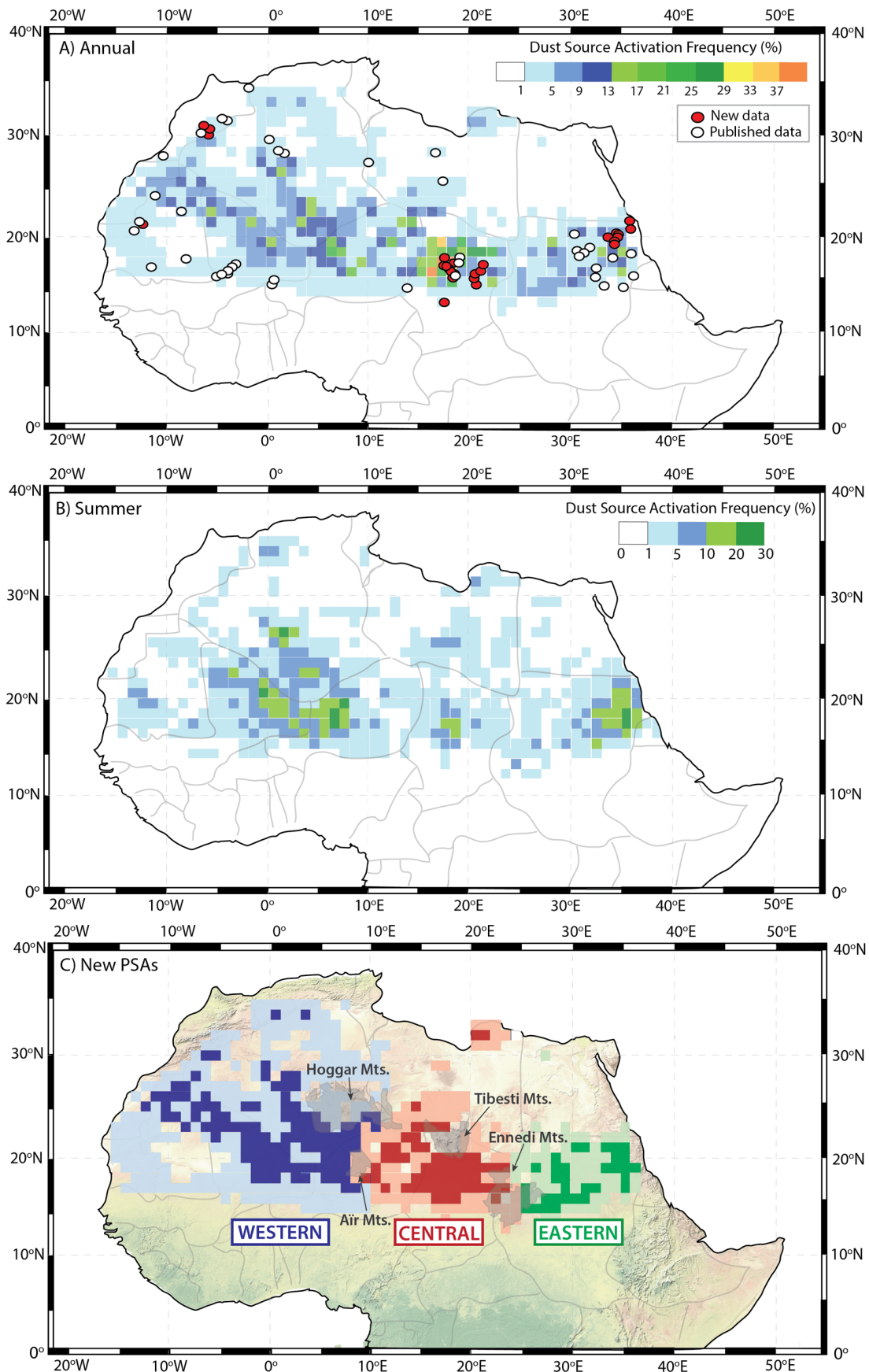


Figure 2: A new analysis revealing three North African preferential dust source areas (PSAs, this study). A) Annual Dust source activation frequency (DSAF) (Schepanski et al., 2012) and location of existing (white circles) and new (red circles, this study) dust source samples with Sr and/or Nd isotope data (published data from Abouchami et al., 2013; Gross et al., 2016; Grousset et al., 1998; Grousset and Biscaye, 2005; Kumar et al., 2014; Padoan et al., 2011; van der Does et al., 2018; Zhao et al., 2018). B) DSAF in boreal summer (JJA) (Schepanski et al., 2007). C) Three new PSAs (this study) based on the data in (A) and the topographic highs used to separate them. Coloured shading denotes annual DSAF > 5% (bold) and DSAF < 5% (pale).

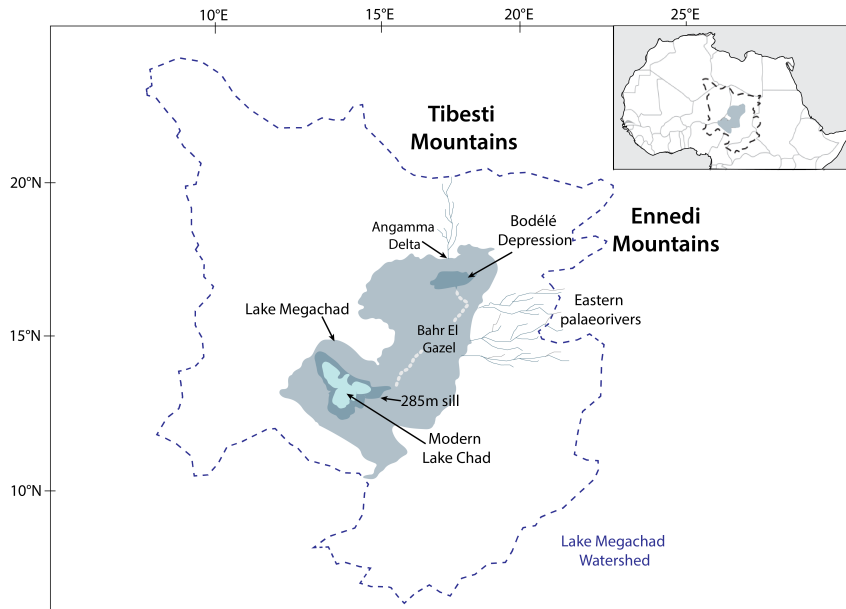


Figure 3: Location, areal extent and palaeohydrology of palaeolake Megachad (adapted from Armitage et al., 2015).

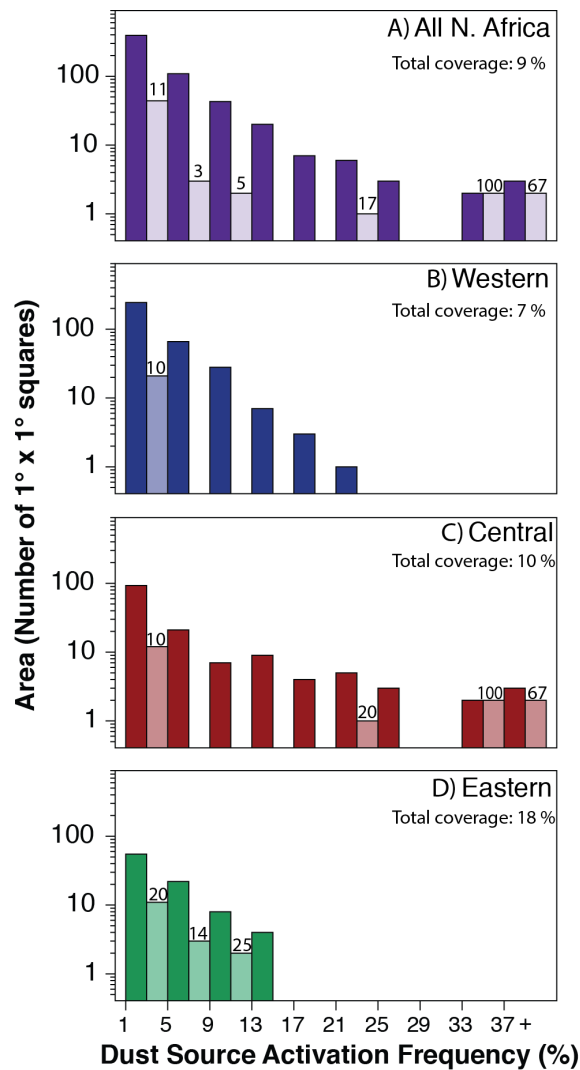


Figure 4: Distribution of dust source activation frequency (DSAF) and isotopic data coverage. Histograms showing the total area (i.e. number of 1° x 1° squares) covered by each DSAF bracket (bold colours, Schepanski et al., 2012) and the corresponding area characterised by isotopic data (pale bars, this study) for A) the whole of North Africa and for the B) Western, C) Central and D) Eastern PSAs. Percentage coverage shown above each bar, and for each PSA.

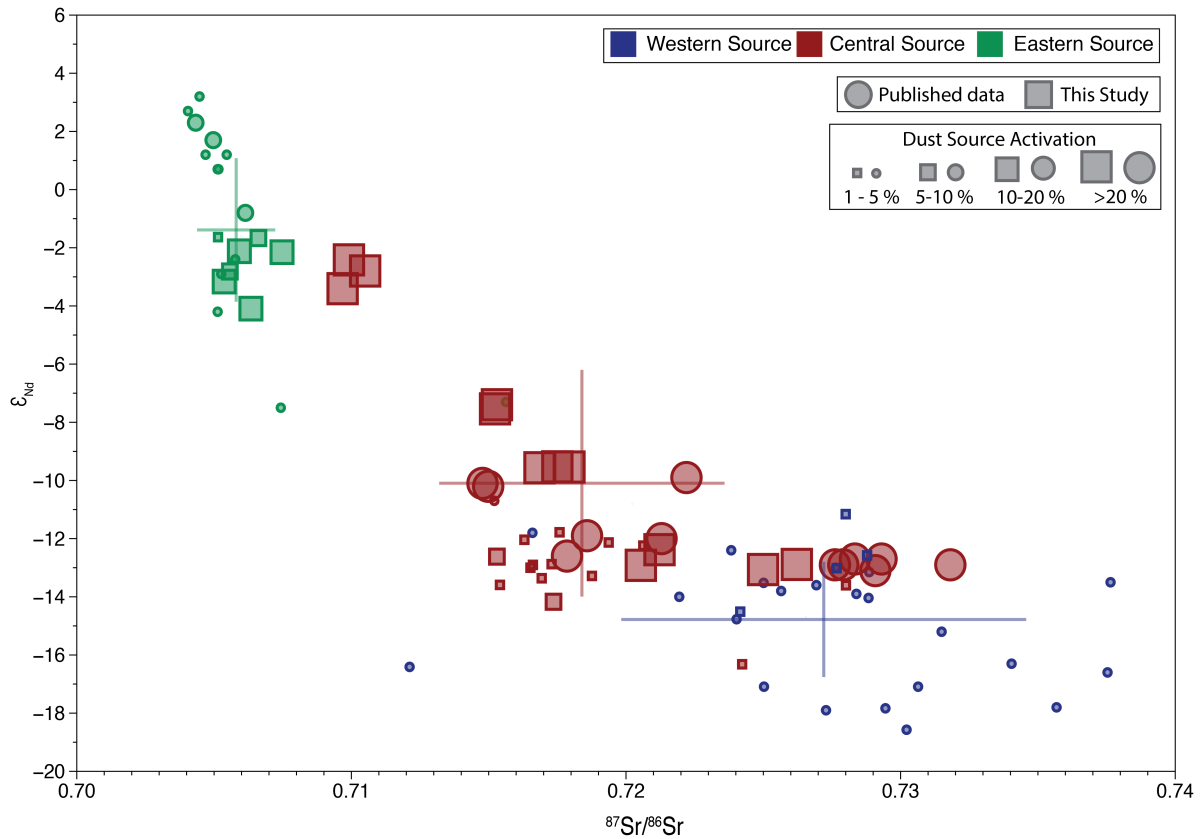


Figure 5: Isotopic composition of our three North African PSAs. New data (squares, this study) and published data (circles) (Abouchami et al., 2013; Gross et al., 2016; Grousset et al., 1998; Grousset and Biscaye, 2005; Kumar et al., 2014; Padoan et al., 2011; Zhao et al., 2018) data from North African dust source regions. Size corresponds to annual DSAF (Schepanski et al., 2012). Crosses denote mean isotopic values for each source region weighted by annual DSAF +/- one weighted standard deviation. Where only ϵ_{Nd} or $^{87}Sr/^{86}Sr$ data is available, sample is not plotted, but the available data still contribute to the weighted PSA mean.

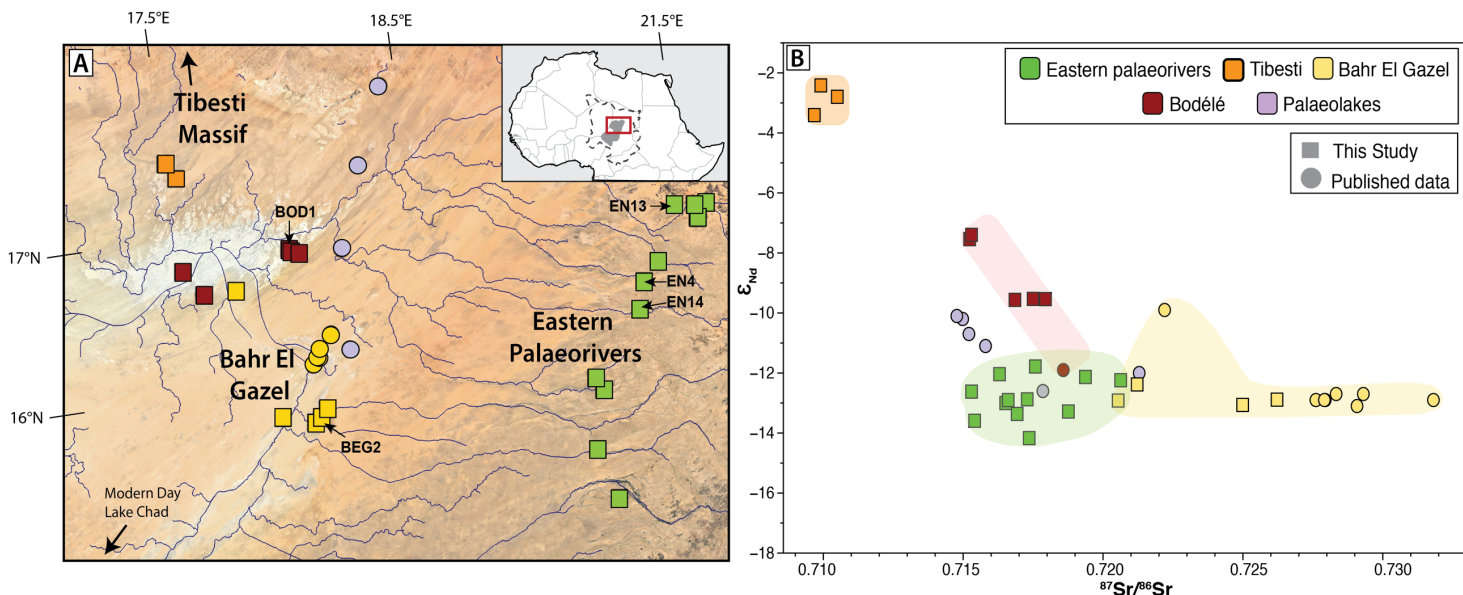


Figure 6: The Chadian region of the central preferential dust source area. A) Sampling locations for new data (squares, this study) and published data (circles, Abouchami et al., 2013; Gross et al., 2016; Grousset and Biscaye, 2005; Kumar et al., 2014) from Chad, in the central PSA. Satellite image taken from Google Earth, overlain with palaeo river reconstructions (Drake and Breeze, 2016). B) Sr and Nd isotope data from Chad, in the Central PSA. Shading highlights main contributors determining the isotopic signature of the Bodélé Depression (red): the Tibesti (orange), Eastern (green) and Bahr El Gazel (yellow) palaeorivers.

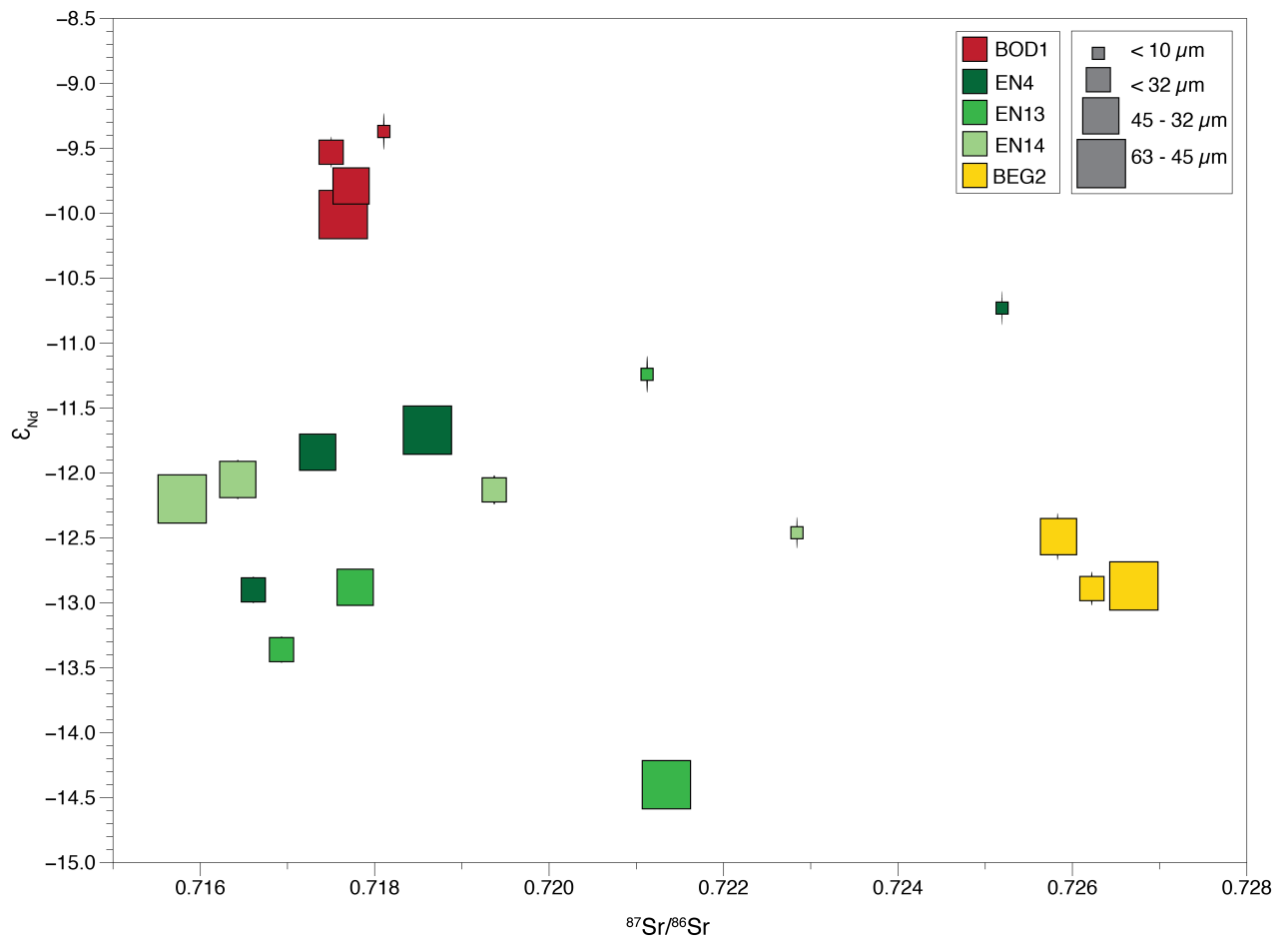


Figure 7: Effect of grain size on Sr and Nd isotopes within the central dust source region. Symbol size denotes grain size (63 - 45 μm , 45 - 32 μm , <32 μm and <10 μm). One sample from each of the Bodélé (BOD1, red) and Bahr El Gazel (BEG2, yellow), and three from the Eastern palaeorivers (EN4, EN13, EN14, green) were analysed. Sample locations shown in Figure 6. Black bars show 2 standard error (often smaller than the symbol). $^{87}\text{Sr}/^{86}\text{Sr}$ for sample BEG2 < 10 μm did not successfully run, but the ϵ_{Nd} is -12.26.

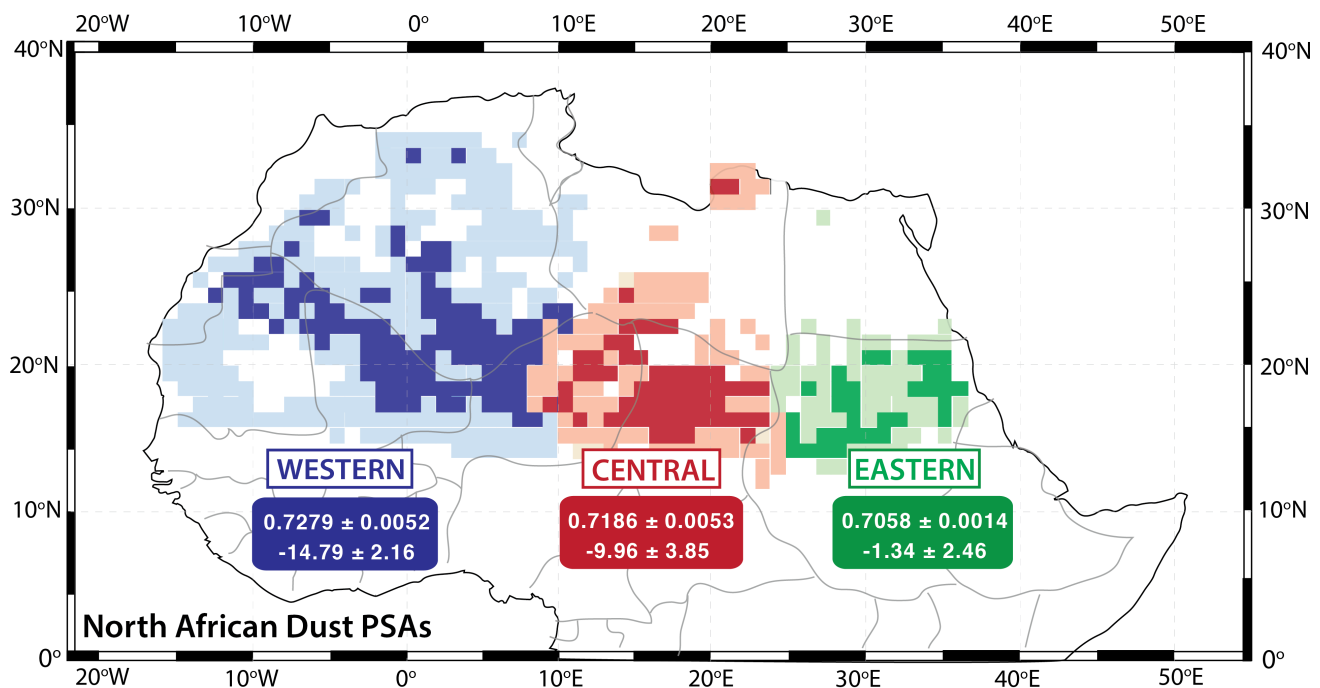


Figure 8: $^{87}\text{Sr}/^{86}\text{Sr}$ (top) and ϵ_{Nd} (bottom) isotope composition of our three North African PSAs (mean values, +/- 1sd, weighted by activation frequency of the source. Dust sources ($1^\circ \times 1^\circ$) with activation frequency > 5% (Schepanski et al., 2012) shown in bold colours, < 5 % in pale colours.

